Reaction Kinetics, Mechanisms and Catalysis (2022) 135:1469–1483
https://doi.org/10.1007/s11144-022-02216-8

Effect of complexation between cobinamides and bovine serum albumin on their reactivity toward cyanide

Ilia A. Dereven'kov[1] · Vladimir S. Osokin[1] · Pavel A. Molodtsov[1] · Anna S. Makarova[1] · Sergei V. Makarov[1]

Received: 20 February 2022 / Accepted: 30 March 2022 / Published online: 4 April 2022

Abstract

Here, we report results of spectrophotometric, spectrofluorimetric, and ultrafiltration studies on the reaction between cobinamides (viz. aquahydroxo-, nitro-, aquacyano- and dicyanocobinamides; Cbi) and bovine serum albumin (BSA), and reactivity of formed complexes toward cyanide. $(H_2O)(HO^-)$Cbi binds BSA at almost equimolar ratio predominantly via amino group of lysine side chains. The mechanism of the reaction involves two steps, i.e. the coordination of amino group on Co(III), and further stabilization of the generated complex. The reaction of $(H_2O)(NO_2^-)$Cbi with BSA is similar with that involving $(H_2O)(HO^-)$Cbi, and both complexes bind cyanide significantly slower than free $(H_2O)(HO^-)$Cbi and $(H_2O)(NO_2^-)$Cbi. $(H_2O)(CN^-)$Cbi binds BSA predominantly via aminogroup as well, however, its coordination proceeds substantially faster and less tightly than in the case of $(H_2O)(HO^-)$Cbi. Binding of $(H_2O)(CN^-)$Cbi and $(H_2O)(HO^-)$Cbi occurs at different sites of BSA as was indicated by spectrofluorimetric titration. Reaction of the complex between $(H_2O)(CN^-)$Cbi and BSA with cyanide proceeds much faster than in the case of the complex between $(H_2O)(HO^-)$Cbi and BSA. $(CN^-)_2$Cbi is partially decyanated by BSA, however, its binding by BSA is relatively low.

Keywords Cobinamide · Vitamin B_{12} · Bovine serum albumin · Cyanide · Complexation

Introduction

Cobalamins (vitamin B_{12}; Cbls) are the ubiquitous cobalt corrin complexes involved in numerous enzymatic processes, i.e. methyl transfer reactions, deoxyadenosyl radical assisted processes, dehalogenation reactions [1] and processes

✉ Ilia A. Dereven'kov
derevenkov@gmail.com

[1] Department of Food Chemistry, Ivanovo State University of Chemistry and Technology, Sheremetevskiy str. 7, Ivanovo, Russia 153000

utilizing S-adenosylmethionine [2]. Besides the role as essential nutrients, Cbls have been successfully examined as antioxidants [3–5]; aquacobalamin (H_2OCbl) is the well-known cyanide antidote [6–9], as well as the other prospective medicinal applications have been reported [10]. Cobinamide (Cbi; Fig. 1) is a nucleotide-free analog of cobalamin. Cbi exhibits a more pronounced effect as cyanide antidote than H_2OCbi [9, 11], that can be partially explained by higher Cbi affinity toward CN^-, i.e. equilibrium constant for CN^- coordination on H_2OCbl is 10^{12} M^{-1} [12], and those for first and second CN^- molecules in the case of the reaction with aquahydroxocobinamide ($(H_2O)(HO^-)Cbi$) are $> 10^{14}$ and ca. 10^8 M^{-1} [12, 13], respectively. Moreover, nitrocobinamide ($(H_2O)(NO_2^-)Cbi$), a complex of Cbi with nitrite, possesses excellent intramuscular adsorption, whereas H_2OCbl can be administered only intravenously [14].

Cobinamides have been examined in other applications as well. $(H_2O)(HO^-)$Cbi readily reacts with hydrogen sulfide via series of coordination and redox steps [15], and its reactivity toward H_2S is superior to that of H_2OCbl [16]. These facts explain successful experiments utilizing Cbi as H_2S antidote [17, 18], whereas H_2OCbl was inefficient in this respect [19]. $(H_2O)(HO^-)$Cbi is efficient as a scavenger of nitric oxide [20]. Nitrosylcobinamide, a complex of one-electron reduced Cbi with nitric oxide, possesses pronounced hypotensive effect [21], and facilitates wound healing [22] and formation of bone tissue [23]. Cobinamides (e.g., $(CN^-)_2$Cbi and its derivatives) have been successfully used to activate soluble guanylyl cyclase [24, 25]. Cbi acts as a redox catalyst as has been shown for dehydroascorbic acid reduction to ascorbic acid by glutathione [26]. Cobinamides are shown to possess antioxidant properties [27].

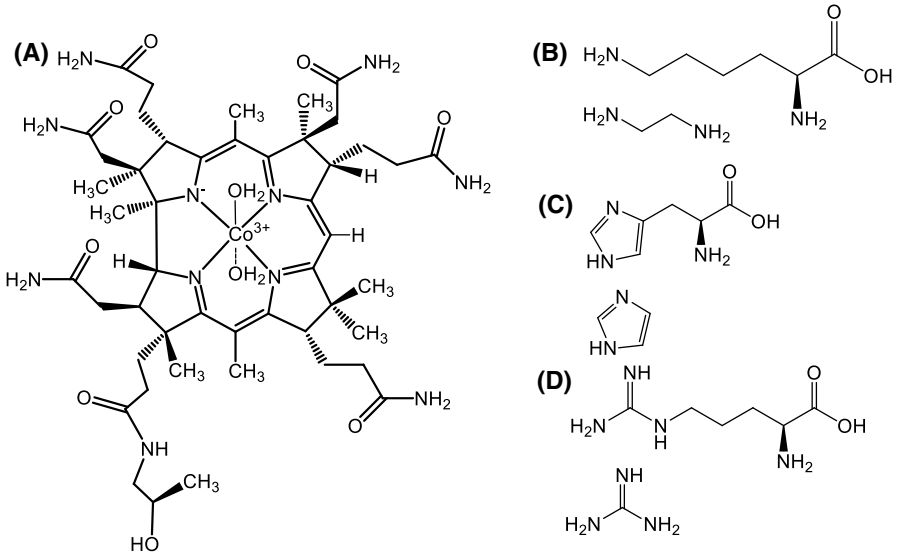

Fig. 1 Structure of diaquacobinamide (**A**), lysine and ethylenediamine (**B**), histidine and imidazole (**C**), and arginine and guanidine (**D**)

Efficacy of corrinoids as cyanide antidotes can be affected by their side reactions with biomolecules. For example, H_2OCbl binds thiocyanate to give thiocyanato-Cbl, which reacts with CN^- more slowly than H_2OCbl, whereas SCN^- does not affect reactivity of $(H_2O)(HO^-)$Cbi toward CN^- [28]. H_2OCbl binds with bovine serum albumin (BSA), a structurally close analog of human serum albumin [29], to give an inert in redox and ligand exchange processes amino complex, which is poorly reactive toward CN^- [30, 31]. Nevertheless, affinity of cobinamides toward serum albumin remains poorly evaluated: it is just reported that $(H_2O)(HO^-)$Cbi tightly binds with BSA [32]. Interaction of $(H_2O)(HO^-)$Cbi with extracellular macromolecules may cause its poor absorption upon intramuscular injection [14, 33]. Here, we report results of study on binding of $(H_2O)(HO^-)$Cbi, $(H_2O)(NO_2^-)$Cbi, $(H_2O)(CN^-)$Cbi and $(CN^-)_2$Cbi with BSA and the reactivity of generated complexes toward cyanide.

Experimental

Cyanocobalamin (vitamin B_{12}; ≥ 98%; Sigma-Aldrich), bovine serum albumin (Sigma; heat shock fraction, pH 5.2; ≥ 96%), sodium borohydride (≥ 98%; Sigma-Aldrich), imidazole (99%; Alfa Aesar), ethylene diamine (99%; Alfa Aesar), sodium nitrite (≥ 98%; Sigma-Aldrich), tyrosine (≥ 98%; Sigma-Aldrich), guanidine hydrochloride (≥ 98%; Sigma-Aldrich), sodium periodate (≥ 99.8%; Sigma), diethyl pyrocarbonate (99%; Sigma-Aldrich), zinc acetate dihydrate (≥ 98%; Sigma-Aldrich) were used as received. Other chemicals were of analytical reagent grade. Buffer solutions (phosphate and the mixture of phosphate and borate; 0.1 M) were used to maintain pH during the measurements.

Synthesis of $(H_2O)(CN^-)$Cbi was performed according to published procedure [34]. Decyanation of $(H_2O)(CN^-)$Cbi included its reduction to Cbi(II) by equal amount of sodium borohydride under anaerobic conditions, acidification of solution by acetic acid to pH 3…4, addition zinc acetate (tenfold excess over $(H_2O)(CN^-)$Cbi) to bind cyanide with Zn^{2+}, and oxidation of Cbi(II) to $(H_2O)_2$Cbi by equal amount of sodium periodate (our earlier experiments indicated that periodate does not modify corrin macrocycle [35]). $(H_2O)_2$Cbi was further purified using column chromatography on silica gel (Sigma-Aldrich; average pore size 60 Å (52–73 Å), 70–230 mesh, 63–200 μm) using 10% aqueous acetic acid as eluent. Identity of product to $(H_2O)_2$Cbi was carried out using ultraviolet–visible (UV–vis spectroscopy; λ_{max}: 349, 496 and 519 nm at pH 7.4 for $(H_2O)(HO^-)$Cbi [28]) and Matrix Assisted Laser Desorption/Ionization-Mass Spectrometry (MALDI-MS; m/z: 990.5 for $[Cbi+H]^+$ ion). Concentrations of corrinoids were determined spectrophotometrically via their conversion to dicyano-species ($\varepsilon_{367} = 30{,}400\ M^{-1}\ cm^{-1}$ [36]). $(H_2O)(NO_2^-)$Cbi and $(CN^-)_2$Cbi were prepared in situ by mixing $(H_2O)_2$Cbi with a twofold excess of sodium nitrite and potassium cyanide, respectively.

Ultraviolet–visible (UV–Vis) spectra were recorded on a cryothermostated (± 0.1 °C) Cary 50 or Shimadzu UV-1800 UV–vis spectrophotometer in quartz cells. Kinetics of rapid reactions was studied on a thermostated (± 0.1 °C) RX2000 (Applied Photophysics, UK) rapid mixing stopped-flow accessory connected to Cary 50 spectrophotometer.

Equilibrium constants were calculated using function A = f([BSA]) derived from Eq. 1 [28]:

$$\frac{A - A_0}{A_\infty - A} = K\left([\text{BSA}] - \frac{A - A_0}{A_\infty - A_0}[\text{Compl.}]\right), \quad (1)$$

Here [BSA] is the total (free + bound) BSA concentration in solution, M; [Compl.] is the total concentration of complex, M; A, A_0, A_∞ are absorbances at the monitoring wavelength for the complex at a particular BSA concentration, for the starting complex, and for the final complex, respectively; K is the equilibrium constant, M^{-1}.

Fluorescence emission spectra were recorded on a Shimadzu RF-6000 spectrofluorophotometer in non-fluorescent cells under aerobic conditions at room temperature (23 ± 2 °C). The excitation wavelength was 280 nm, the excitation and emission bandwidths were 1.5 and 20.0 nm, respectively. The fluorescence intensities were corrected with respect to the inner filter effect [37].

Ultrafiltration experiments were performed using spin-filters with a molecular weight cut-off of 30 kDa (Amicon). Before experiments, spin-filters were first hydrated with 3 mL water by one cycle of centrifugation and then washed by 3 mL of 0.1 M phosphate buffer at 6000 rpm, 10 min in EBA 20 centrifuge (Hettich).

MALDI-MS measurements were performed on Shimadzu AXIMA Confidence mass-spectrometer with 2,5-dihydroxybenzoic acid as the matrix.

pH values of solutions were determined using Multitest IPL-103 pH-meter (SEMICO) equipped with ESK-10601/7 electrode (Izmeritelnaya tekhnika) filled by 3.0 M KCl solution. The electrode was preliminarily calibrated using standard buffer solutions (pH 1.65–12.45).

Results and discussion

Reaction between $(H_2O)(HO^-)$Cbi with bovine serum albumin

Addition of BSA to solution of $(H_2O)(HO^-)$Cbi results in changes in ultraviolet–visible (UV–vis) spectrum shown in Fig. 2 i.e. maxima at 357 and 538 nm are emerged. There was no sharp isosbestic points indicating a presence of several consecutive steps in the reaction mechanism. UV–vis spectrum similar to the spectrum of the product of the reaction between $(H_2O)(HO^-)$Cbi and BSA can be generated via mixing $(H_2O)(HO^-)$Cbi with nitrogenous ligands, i.e. mixing $(H_2O)(HO^-)$Cbi with high excess of ethylene diamine (en) provides maxima at 356 and 536 nm due to the formation of amino complex (Fig. S1), whereas binding of one and two imidazole (ImH) molecules on Co(III)-ion produces species with maxima at 354 and 534 nm and 357 and 541 nm (Fig. S2), respectively. No changes in UV–vis spectrum were observed upon mixing with $(H_2O)(HO^-)$Cbi with tyrosine and guanidine (Figs. S3 and S4). In these experiments, en, ImH and guanidine mimic motifs of lysine, histidine and arginine side chains, respectively (Fig. 1). Therefore, UV–vis spectra provided by Fig. 2 can be attributed to complexation between $(H_2O)(HO^-)$

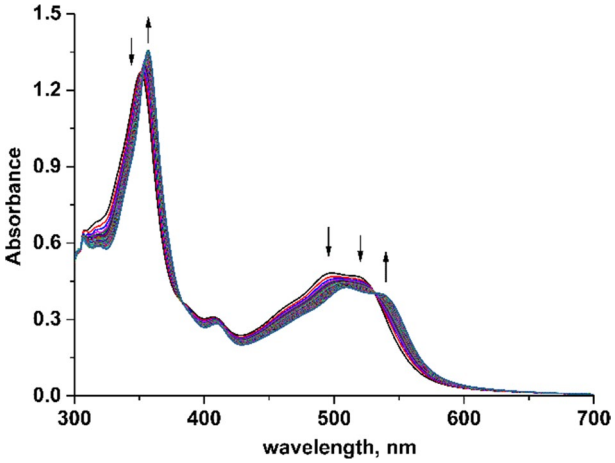

Fig. 2 UV–vis spectra of reaction between $(H_2O)(HO^-)$Cbi (5.0×10^{-5} M) and BSA (1.0×10^{-4} M) at pH 7.4, 25.0 °C

Cbi and nitrogenous group of BSA. It is known that nitrogen atom of histidine can be efficiently ethoxylated by diethyl pyrocarbonate (DEPC) [38]. We modified BSA by tenfold excess of DEPC and compared reactions of $(H_2O)(HO^-)$Cbi with native and ethoxylated BSA. Using DEPC modified BSA, the final product exhibits maximum in UV–vis spectrum at 538 nm slightly less intense than in the case of the reaction with native BSA (Figs. S5 and S6). This results assumes that predominant coordination of Co(III) occurs via lysine amino groups, whereas histidine binding occurs at a lesser extent.

Further, we determined stoichiometry of the reaction by mixing $(H_2O)(HO^-)$Cbi with different quantities of BSA and allowing mixtures to react for 6 h. The results are provided by Fig. 3 indicating complete transformation of $(H_2O)(HO^-)$Cbi to the final product in almost equimolar mixture.

Next, we studied the kinetics of the reaction using an excess of BSA over $(H_2O)(HO^-)$Cbi. The typical kinetic curve of the reaction is shown in Fig. 4. It is described by a two-exponential equation, which can be explained by the presence of two consecutive steps in the system. The dependence of observed rate constants ($k_{obs.}$) on [BSA] for the faster step is linear and exhibits a positive Y-intercept (Fig. 5), that is typical for ligand exchange process. Dividing the value of the slope by the value of the intercept gives value of the equilibrium constant of $7.5\cdot10^3$ M^{-1}, which is far from equimolar binding between reactants. Observed rate constants for the second step of the reaction were poorly reproducible, probably, due to the low contribution of this step in overall UV–vis spectral changes of the reaction in comparison with the first step. Apparently, the second step involves rearrangement of BSA-Cbi complex and increases overall equilibrium constant of the reaction.

The plot of slopes of concentration dependencies of the first step (k') versus pH is shown in Fig. 6. It exhibits sigmoid profile at pH ca. 6.5 and increase at pH > 8. The sigmoid profile can be explained by the protonation of $(H_2O)(HO^-)$Cbi to

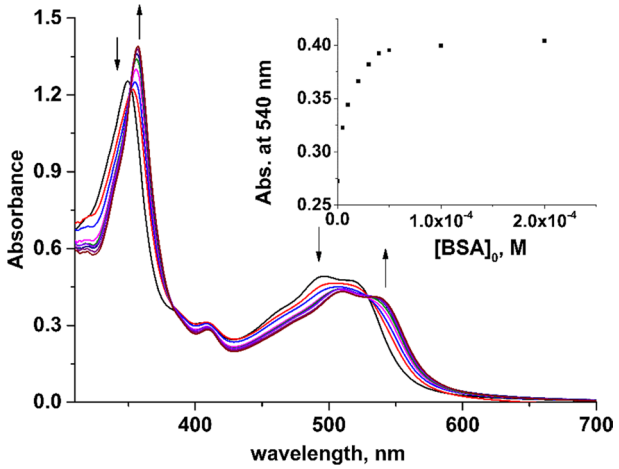

Fig. 3 UV–vis spectra recorded in the course of titration of $(H_2O)(HO^-)$Cbi (5.0×10^{-5} M) by BSA at pH 7.4, 25.0 °C. Inset: a plot of absorbance at 540 nm versus [BSA]

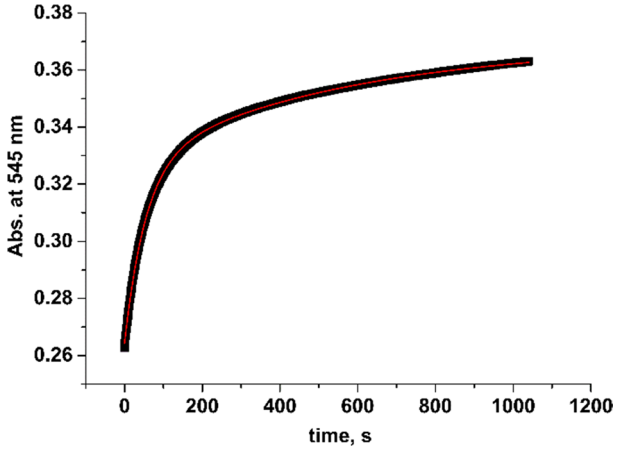

Fig. 4 Kinetic curve of reaction between $(H_2O)(HO^-)$Cbi (5.0×10^{-5} M) and BSA (5.0×10^{-4} M) at pH 7.4, 25.0 °C

$(H_2O)_2$Cbi ($pK_a = 5.9$ at 25 °C [39]), as well as by contribution of histidine binding to Co(III) and its protonation in acidic medium (pK_a ca. 6.6 at 25 °C in proteins [40]). Acceleration of the reaction upon alkalinization is characteristic to the amino group coordination, which is deprotonated in alkaline medium (pK_a ca. 10.5 at 25 °C in proteins [40]). The conversion of $(H_2O)(HO^-)$Cbi to $(HO^-)_2$Cbi is characterized by $pK_a = 10.3$ at 25 °C [39].

Next, we examined complexation between $(H_2O)(HO^-)$Cbi and BSA using fluorescence spectroscopy. Addition of $(H_2O)(HO^-)$Cbi to BSA results in a low quenching of tryptophan fluorescence, whereas prolonged incubation of reactants leads to a

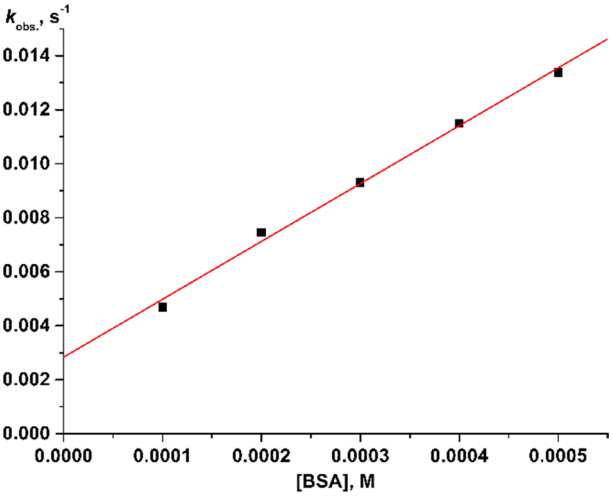

Fig. 5 Plot of $k_{obs.}$ versus [BSA] for the reaction between $(H_2O)(HO^-)$Cbi and BSA at pH 7.4, 25.0 °C

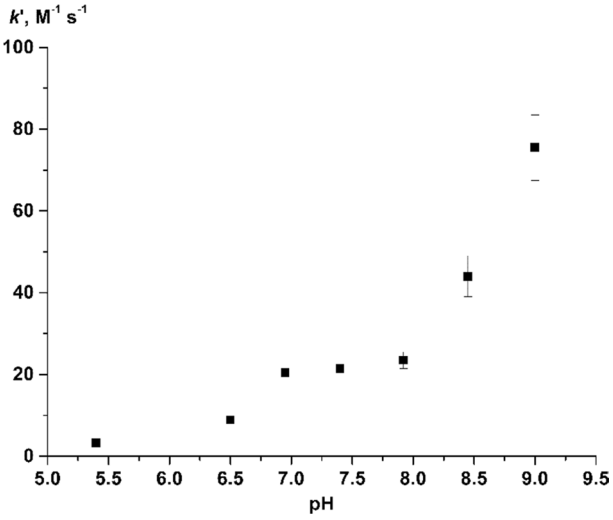

Fig. 6 Plot of *k*' versus pH for the reaction between $(H_2O)(HO^-)$Cbi and BSA at 25.0 °C

deep fluorescence quenching (Fig. S7) that agrees with slow complexation between reactants and formation of weakly fluorescent BSA-Cbi complex.

Strengths of complexation between $(H_2O)(HO^-)$Cbi and BSA was examined by ultrafiltration, since retention of Cbi species by BSA may involve hydrogen bonding, which can be poorly supported by UV–vis and fluorescence data. Although $(H_2O)(HO^-)$Cbi is slightly adsorbed on membrane upon filtration (ca. 10%), its contribution cannot explain significant decrease in cobinamide concentration in permeate in comparison with the initial solution (Fig. S8): i.e. permeate contains ca. 5% ([(H_2O)

$(HO^-)Cbi]_0$:$[BSA]_0$ = 1: 8), ca. 10% ($[(H_2O)(HO^-)Cbi]_0$:$[BSA]_0$ = 1: 1) % of Cbi in comparison with initial solutions. Thus, ultrafiltration supports relatively tight complexation between $(H_2O)(HO^-)$Cbi and BSA, though minor fraction of $(H_2O)(HO^-)$Cbi is weakly bound by BSA and is washed through the membrane in the course of ultrafiltration.

In several experiments, cobinamides are administered as cyanide antidotes prior to the toxin introduction [41], thus, we tested the influence of $(H_2O)(HO^-)$Cbi binding with BSA on its reactivity toward cyanide. Addition of CN^- to $(H_2O)(HO^-)$Cbi results in the rapid formation of $(CN^-)_2$Cbi exhibiting maxima at 367, 540 and 580 nm (Fig. S9). In the case of complex between BSA and Cbi, generation of $(CN^-)_2$Cbi occurs significantly slower: although the minor fraction of $(CN^-)_2$Cbi is formed within 1 min after addition of CN^-, complete transformation complex between Cbi and BSA to $(CN^-)_2$Cbi is not observed for 2 h of the reaction (Fig. 7).

Despite the high reactivity of $(H_2O)(HO^-)$Cbi toward CN^-, it is rarely used in experiments as antidote due to certain toxicity [20]. This drawback can be eliminated by using $(H_2O)(HO^-)$Cbi derivatives (e.g. nitrocobinamide; $(H_2O)(NO_2^-)$Cbi). Thus, we examined $(H_2O)(NO_2^-)$Cbi reaction with BSA as well. Changes in UV–vis spectrum of the reaction between $(H_2O)(NO_2^-)$Cbi and BSA are shown in Fig. S10, i.e. the same product is formed as in the case of reaction of $(H_2O)(HO^-)$Cbi with BSA. Thus, nitrite molecule in $(H_2O)(NO_2^-)$Cbi is substituted by one of BSA amino groups. Binding of $(H_2O)(NO_2^-)$Cbi to BSA is accompanied by quenching of tryptophan fluorescence (Fig. S11) as in the case of the reaction involving $(H_2O)(HO^-)$Cbi. Data shown in Fig. S12 indicate that significant fraction of $(H_2O)(NO_2^-)$Cbi is retained by BSA upon ultrafiltration, i.e. permeate contains ca. 5% ($[(NO_2^-)Cbi]_0$:$[BSA]_0$ = 1: 8), ca. 15% ($[(NO_2^-)Cbi]_0$:$[BSA]_0$ = 1: 1) % of Cbi in comparison with initial solutions, whereas membrane adsorbs ca. 12% of (H_2O)

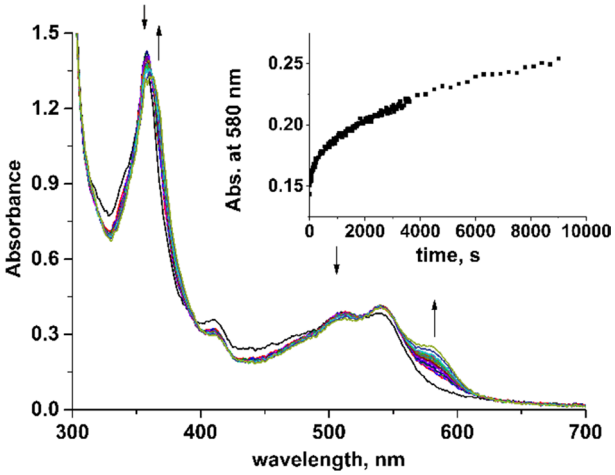

Fig. 7 UV–vis spectra collected after mixing complex between $(H_2O)(HO^-)$Cbi ($[(H_2O)(HO^-)Cbi]_0 = 5.0\times10^{-5}$ M) and BSA ($[BSA]_0 = 4.0\times10^{-4}$ M) with CN^- (1.0×10^{-4}) at pH 7.4, 25.0 °C. Inset: a time-course curve of the reaction

(NO_2^-)Cbi. Binding of (H_2O)(NO_2^-)Cbi to BSA decreases its reactivity toward CN^- as well: complex cannot be transformed completely to (CN^-)$_2$Cbi for 2 h, although the major fraction of CN^- binds to cobinamide within ca. 2 min (i.e. faster than in the case of the reaction involving the complex between (H_2O)(HO^-)Cbi and BSA).

Reaction between (H_2O)(CN^-)Cbi with bovine serum albumin

Mixing of (H_2O)(CN^-)Cbi with BSA produces complex with absorption maxima at 360, 520 and 549 nm (Fig. 8). It proceeds faster than complexation of (H_2O)(HO^-)Cbi with BSA, i.e. for several seconds and hundreds of seconds in the case of ((H_2O)(CN^-)Cbi and ((H_2O)(HO^-)Cbi, respectively (pH 7.4, 25.0 °C). The final product of the reaction between (H_2O)(CN^-)Cbi and BSA exhibits spectrum, which is close to those of (en)(CN^-)Cbi (λ_{max}: 359, 519 and 547 nm; Fig. S14) and (ImH)(CN^-)Cbi (λ_{max}: 360, 519 and 552 nm; Fig. S15). Tyrosine and guanidine do not react with (H_2O)(CN^-)Cbi (Figs. S16 and S17). Modification of BSA by DEPC slightly decreases intensity of peaks at 520 and 549 nm in UV–vis spectrum of reaction product (Fig. S18) indicating formation of minor fraction of BSA(histidine)–(CN^-)Cbi complex and predominance of BSA(lysine)–(CN^-)Cbi form.

In contrast to binding of (H_2O)(HO^-)Cbi, the complexation between (H_2O)(CN^-)Cbi and BSA occurs more weakly and requires ca. tenfold excess of BSA over (H_2O)(CN^-)Cbi to completely convert it to bound state (Fig. 9). Fitting the plot of absorbance at 555 nm versus [BSA] to Eq. 1 gives value of equilibrium constant $K = (6.9 \pm 0.6) \times 10^3\ M^{-1}$ (pH 7.4, 25.0 °C).

Typical kinetic curve of the reaction between (H_2O)(CN^-)Cbi and an excess of BSA is shown in Fig. 10. It is described by exponential equation indicating the first order with respect to cobinamide. The plot of observed rate constants versus [BSA]

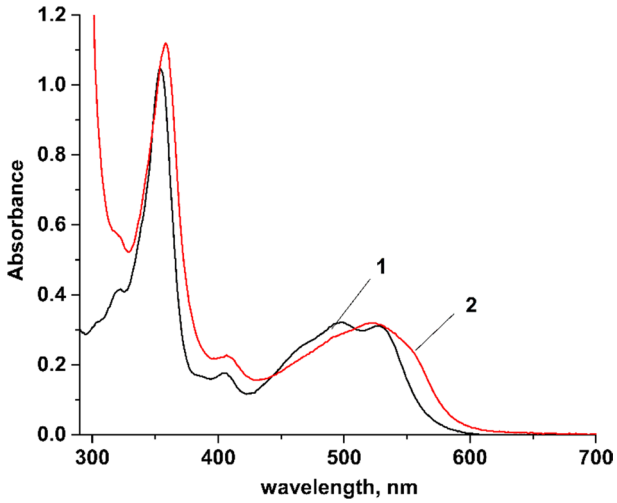

Fig. 8 UV–vis spectra recorded before (1) and after (2) mixing of (H_2O)(CN^-)Cbi (4.0×10^{-5} M) and BSA (3.3×10^{-4} M) at pH 7.4, 25.0 °C

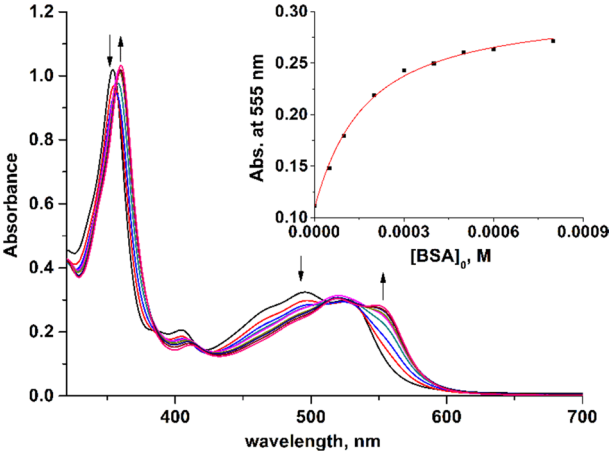

Fig. 9 UV–vis spectra recorded in the course of titration of $(H_2O)(CN^-)$Cbi (3.9×10^{-5} M) by BSA at pH 7.4, 25.0 °C. Inset: a plot of absorbance at 555 nm versus [BSA] fitted to Eq. 1

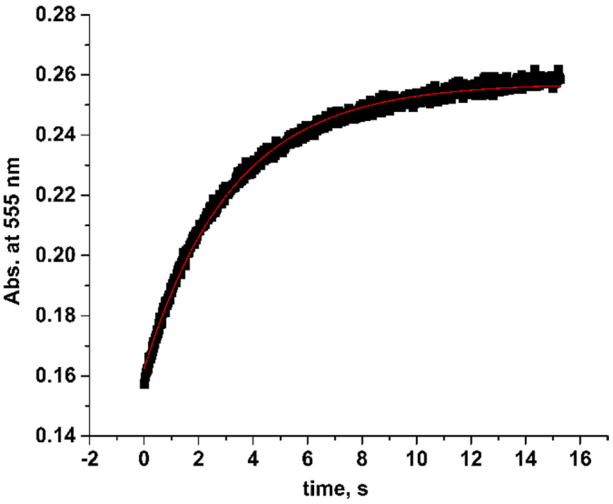

Fig. 10 Kinetic curve of reaction between $(H_2O)(CN^-)$Cbi (4.0×10^{-5} M) and BSA (4.0×10^{-4} M) at pH 7.4, 25.0 °C

is linear and shows a positive Y-intercept (Fig. 11) that is typical to the reversible complexation between reactants. Dividing the value of the slope by the value of the intercept gives value of the equilibrium constant $K = 5.9\cdot10^3$ M^{-1}, which agrees with the value obtained by the titration ($6.9\cdot10^3$ M^{-1}).

Dependence of the rate constant of the forward reaction between $(H_2O)(CN^-)$Cbi and BSA on pH (Fig. 12) is similar to that involving $(H_2O)(HO^-)$Cbi (Fig. 6) with the exception of the absence of sigmoid profile in a near neutral region. Conversion of $(H_2O)(CN^-)$Cbi to $(HO^-)(CN^-)$Cbi is characterized by $pK_a = 11.0$

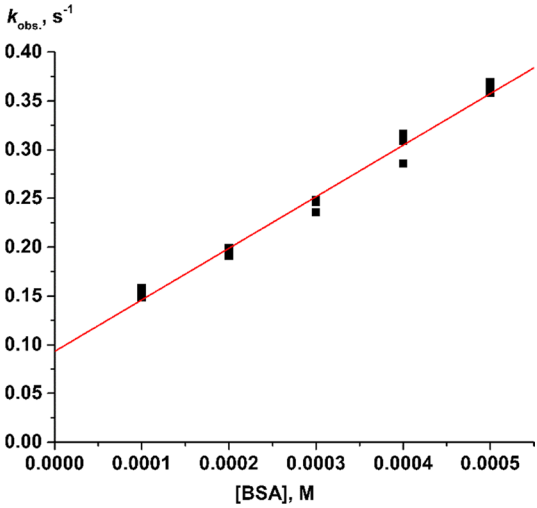

Fig. 11 Plot of $k_{obs.}$ versus [BSA] for the reaction between $(H_2O)(CN^-)$Cbi and BSA at pH 7.4, 25.0 °C

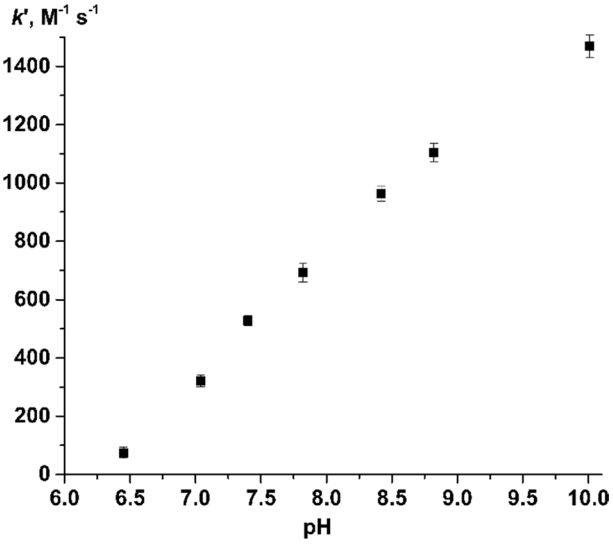

Fig. 12 Plot of k' versus pH for the reaction between $(H_2O)(CN^-)$Cbi and BSA at 25.0 °C

(25 °C) [42]. Thus, increase of rate upon alkalinization corresponds to deprotonation of lysine residues to the more reactive NH_2-form.

Complexation between $(H_2O)(CN^-)$Cbi and BSA results in a weak tryptophan fluorescence quenching (Fig. S19), that is distinct from substantially deeper quenching effects of $(H_2O)(HO^-)$Cbi (Fig. S7) and $(NO_2^-)_2$Cbi (Fig. S11). These observations can be explained by different binding sites of $(H_2O)(CN^-)$Cbi and $(H_2O)(HO^-)$Cbi or $(NO_2^-)_2$Cbi in BSA molecule. In the case of $(H_2O)(HO^-)$Cbi

and $(NO_2^-)_2$Cbi, the binding site is located closer to BSA tryptophan residue than for $(H_2O)(CN^-)$Cbi.

Using ultrafiltration experiments (Fig. S20), we showed that $(H_2O)(CN^-)$Cbi retention by BSA is substantial in the case of a eightfold excess of BSA over $(H_2O)(CN^-)$Cbi (i.e. permeate contains ca. 8% of initial Cbi concentration) and becomes lower in the equimolar mixture (i.e. Cbi concentration in permeate is ca. 35% of the initial concentration). Binding of free $(H_2O)(CN^-)$Cbi on the membrane is ca. 8%.

We found that binding of $(H_2O)(CN^-)$Cbi by BSA slightly decreases rate of the reaction with CN^- (Fig. S21), however, the reaction is substantially faster than processes involving complexes of BSA with $(H_2O)(HO^-)$Cbi (Fig. 7) or $(NO_2^-)_2$Cbi (Fig. S13).

$(CN^-)_2$Cbi reacts with BSA as well (Fig. 13). The reaction is accompanied by slow gradual decrease of absorbance at 580 nm due to its partial decyanation. The reaction results in a slight tryptophan fluorescence quenching (Fig. S22), which is comparable with that observed for $(H_2O)(CN^-)$Cbi (Fig. S19).

Ultrafiltration experiments indicate that $(CN^-)_2$Cbi concentration in permeate is ca. 25% of the initial in the case of an eightfold excess of BSA and ca. 35% of the initial in the case of the equimolar mixture (Fig. S23). $(CN^-)_2$Cbi binding by membrane is ca. 15%. Therefore, introduction of tightly bound ligands to cobinamide decreases its retention by BSA. However, ultrafiltration data shows that weak complexation between $(CN^-)_2$Cbi and BSA occurs and is contributed probably by hydrogen bonding.

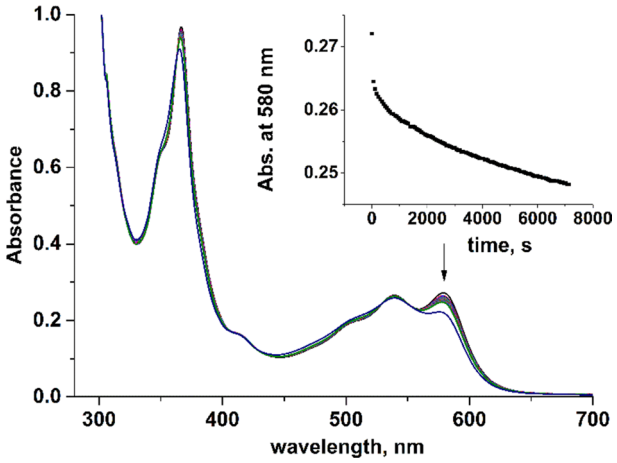

Fig. 13 UV–vis spectra collected for the reaction between $(CN^-)_2$Cbi ($[(CN^-)_2Cbi]_0 = 3.0 \times 10^{-5}$ M) and BSA ($[BSA]_0 = 4.0 \times 10^{-4}$ M) at pH 7.4, 25.0 °C. Time interval between spectra is 1 min, the final spectrum was recorded after 24 h of incubation. Inset: a time-course curve of the reaction

Conclusions

This work showed for the first time that cobinamide species are reactive toward proteins. Thus, bovine serum albumin binds $(H_2O)(HO^-)$Cbi, $(H_2O)(NO_2^-)$Cbi and $(H_2O)(CN^-)$Cbi predominantly via aminogroups of lysine residues, as well as the minor fraction exists as the histidine complex. In the case of $(H_2O)(HO^-)$Cbi, binding occurs in equimolar ratio. Upon binding with BSA, the reactivity of $(H_2O)(HO^-)$Cbi and $(H_2O)(NO_2^-)$Cbi toward cyanide is substantially decreased, although rate of CN^- binding is higher in the case of nitro-Cbi-BSA complex that may partially explain why $(H_2O)(NO_2^-)$Cbi is used more frequently as CN^- antidote than $(H_2O)(HO^-)$Cbi. These results suggest that introduction of Cbi might be more efficient after cyanide poisoning than prior this event to prevent the formation of inert complex between Cbi and BSA. The binding of $(H_2O)(CN^-)$Cbi is much weaker than of $(H_2O)(HO^-)$Cbi, and sustains relatively high reactivity toward CN^-. Moreover, binding of $(H_2O)(CN^-)$Cbi and $(H_2O)(HO^-)$Cbi occurs at different sites of BSA as was indicated by spectrofluorimetric titration. $(CN^-)_2$Cbi is the least reactive toward BSA Cbi species studied in this work, and is poorly retained by BSA.

Supplementary Information The online version contains supplementary material available at https://doi.org/10.1007/s11144-022-02216-8.

Funding This work was supported by the Russian Science Foundation (Project No. 21-73-10057, https://rscf.ru/project/21-73-10057/) to IAD. The study was carried out using the resources of the Center for Shared Use of Scientific Equipment of the ISUCT (with the support of the Ministry of Science and Higher Education of Russia, Grant No. 075-15-2021-671).

Declarations

Conflict of interest The authors declare that they have no conflict of interest.

References

1. Brown KL (2005) Chemistry and enzymology of vitamin B_{12}. Chem Rev 105:2075–2149. https://doi.org/10.1021/cr030720z
2. Bridwell-Rabb J, Grell TAJ, Drennan CL (2018) A rich man, poor man story of S-adenosylmethionine and cobalamin revisited. Annu Rev Biochem 87:555–584. https://doi.org/10.1146/annurev-biochem-062917-012500
3. Birch CS, Brasch NE, McCaddon A, Williams JHH (2009) A novel role for vitamin B_{12}: cobalamins are intracellular antioxidants in vitro. Free Radic Biol Med 47:184–188. https://doi.org/10.1016/j.freeradbiomed.2009.04.023
4. Moreira ES, Brasch NE, Yun J (2011) Vitamin B_{12} protects against superoxide-induced cell injury in human aortic endothelial cells. Free Radic Biol Med 51:876–883. https://doi.org/10.1016/j.freeradbiomed.2011.05.034
5. Chan W, Almasieh M, Catrinescu M-M, Levin LA (2018) Cobalamin-associated superoxide scavenging in neuronal cells is a potential mechanism for vitamin B_{12}–deprivation optic neuropathy. Am J Pathol 188:160–172. https://doi.org/10.1016/j.ajpath.2017.08.032
6. Forsyth JC, Mueller PD, Becker CE et al (1993) Hydroxocobalamin as a cyanide antidote: safety, efficacy and pharmacokinetics in heavily smoking normal volunteers. J Toxicol Clin Toxicol 31:277–294. https://doi.org/10.3109/15563659309000395

7. Borron SW, Baud FJ, Mégarbane B, Bismuth C (2007) Hydroxocobalamin for severe acute cyanide poisoning by ingestion or inhalation. Am J Emerg Med 25:551–558. https://doi.org/10.1016/j.ajem.2006.10.010
8. Thompson JP, Marrs TC (2012) Hydroxocobalamin in cyanide poisoning. Clin Toxicol 50:875–885. https://doi.org/10.3109/15563650.2012.742197
9. Bebarta VS, Tanen DA, Boudreau S et al (2014) Intravenous cobinamide versus hydroxocobalamin for acute treatment of severe cyanide poisoning in a swine (*Sus scrofa*) model. Ann Emerg Med 64:612–619. https://doi.org/10.1016/j.annemergmed.2014.02.009
10. Zelder F (2015) Recent trends in the development of vitamin B_{12} derivatives for medicinal applications. Chem Commun 51:14004–14017. https://doi.org/10.1039/C5CC04843E
11. Brenner M, Mahon SB, Lee J et al (2010) Comparison of cobinamide to hydroxocobalamin in reversing cyanide physiologic effects in rabbits using diffuse optical spectroscopy monitoring. J Biomed Opt 15:017001. https://doi.org/10.1117/1.3290816
12. Hayward GC, Hill HAO, Pratt JM et al (1965) The chemistry of vitamin B12. Part IV. The thermodynamic trans-effect. J Chem Soc. https://doi.org/10.1039/JR9650006485
13. George P, Irvine DH, Glauser SC (1960) The influence of chelation in determining the reactivity of the iron in hemoproteins, and the cobalt in vitamin B_{12} derivatives. Ann N Y Acad Sci 88:393–415. https://doi.org/10.1111/j.1749-6632.1960.tb20038.x
14. Chan A, Jiang J, Fridman A et al (2015) Nitrocobinamide, a new cyanide antidote that can be administered by intramuscular injection. J Med Chem 58:1750–1759. https://doi.org/10.1021/jm501565k
15. Salnikov DS, Makarov SV, van Eldik R et al (2014) Kinetics and mechanism of the reaction of hydrogen sulfide with diaquacobinamide in aqueous solution. Eur J Inorg Chem. https://doi.org/10.1002/ejic.201402082
16. Salnikov DS, Kucherenko PN, Dereven'kov IA et al (2014) Kinetics and mechanism of the reaction of hydrogen sulfide with cobalamin in aqueous solution. Eur J Inorg Chem. https://doi.org/10.1002/ejic.201301340
17. Ng PC, Hendry-Hofer TB, Garrett N et al (2019) Intramuscular cobinamide versus saline for treatment of severe hydrogen sulfide toxicity in swine. Clin Toxicol 57:189–196. https://doi.org/10.1080/15563650.2018.1504955
18. Brenner M, Benavides S, Mahon SB et al (2014) The vitamin B_{12} analog cobinamide is an effective hydrogen sulfide antidote in a lethal rabbit model. Clin Toxicol 52:490–497. https://doi.org/10.3109/15563650.2014.904045
19. Bebarta VS, Garrett N, Brenner M et al (2017) Efficacy of intravenous cobinamide versus hydroxocobalamin or saline for treatment of severe hydrogen sulfide toxicity in a swine (*Sus scrofa*) model. Acad Emerg Med 24:1088–1098. https://doi.org/10.1111/acem.13213
20. Broderick KE, Singh V, Zhuang S et al (2005) Nitric oxide scavenging by the cobalamin precursor cobinamide. J Biol Chem 280:8678–8685. https://doi.org/10.1074/jbc.M410498200
21. Broderick KE, Alvarez L, Balasubramanian M et al (2007) Nitrosyl-cobinamide, a new and direct nitric oxide releasing drug effective in vivo. Exp Biol Med 232:1432–1440. https://doi.org/10.3181/0703-rm-70
22. Spitler R, Schwappacher R, Wu T et al (2013) Nitrosyl-cobinamide (NO-Cbi), a new nitric oxide donor, improves wound healing through cGMP/cGMP-dependent protein kinase. Cell Signal 25:2374–2382. https://doi.org/10.1016/j.cellsig.2013.07.029
23. Kalyanaraman H, Ramdani G, Joshua J et al (2017) Direct NO donor regulates osteoblast and osteoclast functions and increases bone mass in ovariectomized mice. J Bone Miner Res 32:46–59. https://doi.org/10.1002/jbmr.2909
24. Ó Proinsias K, Giedyk M, Sharina IG et al (2012) Synthesis of new hydrophilic and hydrophobic cobinamides as NO independent sGC activators. ACS Med Chem Lett 3:476–479. https://doi.org/10.1021/ml300060n
25. Sharina I, Sobolevsky M, Doursout M-F et al (2012) Cobinamides are novel coactivators of nitric oxide receptor that target soluble guanylyl cyclase catalytic domain. J Pharmacol Exp Ther 340:723–732. https://doi.org/10.1124/jpet.111.186957
26. Dereven'kov IA, Makarov SV, Bui Thi TT et al (2018) Studies on the reduction of dehydroascorbic acid by glutathione in the presence of aquahydroxocobinamide. Eur J Inorg Chem. https://doi.org/10.1002/ejic.201800066

27. Schwaerzer GK, Kalyanaraman H, Casteel DE et al (2019) Aortic pathology from protein kinase G activation is prevented by an antioxidant vitamin B_{12} analog. Nat Commun 10:3533. https://doi.org/10.1038/s41467-019-11389-1
28. Dereven'kov IA, Salnikov DS, Makarov SV et al (2013) Comparative study of reaction of cobalamin and cobinamide with thiocyanate. J Inorg Biochem 125:32–39. https://doi.org/10.1016/j.jinorgbio.2013.04.011
29. Bujacz A (2012) Structures of bovine, equine and leporine serum albumin. Acta Cryst D 68:1278–1289. https://doi.org/10.1107/S0907444912027047
30. Dereven'kov IA, Hannibal L, Makarov SV et al (2018) Characterization of the complex between native and reduced bovine serum albumin with aquacobalamin and evidence of dual tetrapyrrole binding. J Biol Inorg Chem 23:725–738. https://doi.org/10.1007/s00775-018-1562-8
31. Dereven'kov IA, Makarov SV, Molodtsov PA (2020) Effect of bovine serum albumin on redox and ligand exchange reactions involving aquacobalamin. Macroheterocycles 13:223–228. https://doi.org/10.6060/mhc200498d
32. Taylor RT, Hanna M (1970) Binding of aquocobalamin to the histidine residues in bovine serum albumin. Arch Biochem Biophys 141:247–257. https://doi.org/10.1016/0003-9861(70)90129-3
33. Hendry-Hofer TB, Ng PC, McGrath AM et al (2020) Intramuscular aminotetrazole cobinamide as a treatment for inhaled hydrogen sulfide poisoning in a large swine model. Ann NY Acad Sci 1479:159–167. https://doi.org/10.1111/nyas.14339
34. Zhou K, Zelder F (2011) One-step synthesis of α/β cyano-aqua cobinamides from vitamin B_{12} with Zn(II) or Cu(II) salts in methanol. J Porphyr Phthalocyanines 15:555–559. https://doi.org/10.1142/S1088424611003446
35. Dereven'kov IA, Shpagilev NI, Makarov SV (2018) Mechanism of the reaction between cobalamin(II) and periodate. Russ J Phys Chem A 92:2182–2186. https://doi.org/10.1134/S0036024418110080
36. Barker HA, Smyth RD, Weissbach H et al (1960) Isolation and properties of crystalline cobamide coenzymes containing benzimidazole or 5,6-dimethylbenzimidazole. J Biol Chem 235:480–488. https://doi.org/10.1016/S0021-9258(18)69550-X
37. Macii F, Biver T (2021) Spectrofluorimetric analysis of the binding of a target molecule to serum albumin: tricky aspects and tips. J Inorg Biochem 216:111305. https://doi.org/10.1016/j.jinorgbio.2020.111305
38. Mendoza VL, Vachet RW (2009) Probing protein structure by amino acid-specific covalent labeling and mass spectrometry. Mass Spectrom Rev 28:785–815. https://doi.org/10.1002/mas.20203
39. Baidwin DA, Betterton EA, Pratt JM (1983) The chemistry of vitamin B12. Part 20. diaquocobinamide: pK values and evidence for conformational isomers. J Chem Soc Dalton Trans. https://doi.org/10.1039/DT9830000217
40. Grimsley GR, Scholtz JM, Pace CN (2009) A summary of the measured pK values of the ionizable groups in folded proteins. Protein Sci 18:247–251. https://doi.org/10.1002/pro.19
41. Chan A, Balasubramanian M, Blackledge W et al (2010) Cobinamide is superior to other treatments in a mouse model of cyanide poisoning. Clin Toxicol 48:709–717. https://doi.org/10.3109/15563650.2010.505197
42. Marques HM, Bradley JC, Brown KL, Brooks H (1993) Placing hydroxide in the thermodynamic tram influence order of the cobalt corrinoids: equilibrium constants for the reaction of some ligands with aquahydroxocobinamide. Inorg Chim Acta 209:161–169. https://doi.org/10.1016/S0020-1693(00)85137-3